Engineering Solid Mechanics 11 (2023) 135-150

Contents lists available at GrowingScience

Engineering Solid Mechanics

homepage: www.GrowingScience.com/esm

Orthotropic plates with dynamic vertical seismic load modeled as multi line

Toni Hartono Bagio[a*], Sofia W. Alisjahbana[b], Helmy Darjanto[c] and Najid Najid[a]

[a]*Civil Engineering Department, Faculty of Engineering, Universitas Tarumanagara , Jakarta 11440, Indonesia*
[b]*Civil Engineering Department, Bakrie University, Jakarta 12420, Indonesia*
[c]*Department of Civil Engineering, Narotama University, Surabaya, Indonesia*

ARTICLEINFO

Article history:
Received 20 September 2022
Accepted 12 January 2023
Available online
12 January 2023

Keywords:
Bovo-Sovoia's modified
Multiline
Quadratic and sextic equation
Boundary condition ES (Elastic Support)
ER (Elastic Restraint)
ESR (Elastic Support and Restraint)
PGAv (Vertical Peak Ground Acceleration)
Modified Bolotin Method
Auxiliary Levy

ABSTRACT

Calculation plate floor concrete, using a static load which is a gravity load consisting of a live load and a dead load, with various of boundary conditions, floor slabs are orthotropic plate, and rarely account for dynamic loads due to vertical seismic loads, with other boundary conditions, such as Clamped, simply supported, ES (Elastic Support), ER (Elastic Restraint), and ESR (Elastic Support and Restraint). Analytical solution based on the Modified Bolotin Method to analyze floor slab under Vertical Peak Ground Acceleration (PGAv), the natural frequency solution based on auxiliary Levy's type problems. Dynamic vertical seismic loads using multiline, first line at $0 \le t < 0.5$ is linear equation, second line at $0.05 \le t \le 0.15$ is quadratic equation, third line $0.15 < t \le 0.6$ is sextic equation, last line, $t > 0.6$ is linear equation, vertical seismic load with two conditions far fault and near fault, multi-line equation are depending on (*PGAv/g*). A numerical example is given, for various boundary conditions, and far fault, translational stiffness (k_x, k_y) and rotational stiffness (c_x, c_y), from the results of plate calculations due to dynamic vertical seismic loads with 5 types of edge support, ES (elastic support) is the best result.

1. Introduction

Reinforcement of concrete slabs, usually very simple, this is due to deflection limitations, for concrete floor slabs with an area below 10 m², it is almost certain to use minimum reinforcement with a minimum thickness of 120 mm. However, if the slab area is greater than 10 m², it is certain that more reinforcement is needed than the minimum required. Calculation of moments on concrete slabs, often using tables (ACI 318-63, 1963), (PBI, 1971), (BS8110, 1997), Indonesian whereas Indonesian Concrete Code 2019 (SNI 2847:19, 2019), as well as American Concrete Code (ACI-318M-14, 2014) do not include detailed plate calculations, but use the direct design method or equivalent frame method. Another limitation is regarding the assumption of support on all four sides, in whereas Indonesian Concrete Code 1971(PBI, 1971), consisting of fully clamped, elastically clamped, and free conditions, where the assumption of fully clamped does not match the actual conditions in the field, which is not really clamped. In the discussion above, all loads acting on the plates are only based on static loads, which are gravity loads consisting of dead loads and live loads, and the edge support used is a clamped and simple support. Even though the loads acting on the plates are not only static loads, but also dynamic loads, where the dynamic loads are seismic loads, which act on the x, y and z axes. The x-axis and y-axis are horizontal earthquake loads while the z-axis is vertical seismic loads. Vertical seismic load, which are dynamic loads on the plates, the relationship between vertical seismic loads and gravitational loads has just been studied by Bovo-Savoia)(Bovo & Savoia, 2019), provide the Vertical Peak Ground Acceleration (PGAv) (Berkeley.edu, n.d.)

* Corresponding author.
E-mail addresses: tony@narotama.ac.id (T. H. Bagio)

ISSN 2291-8752 (Online) - ISSN 2291-8744 (Print)

doi: 10.5267/j.esm.2023.1.002

The dynamic response of rigid roadway pavements (Alisjahbana & Wangsadinata, 2015), subjected to dynamic loads, such as vehicle loads to the design of rigid pavement (Zhu & Law, 2003). Boundary conditions for simply supported (Vijayakumar, 1974), for clamped (Elishakoff, 1974; Vijayakumar & Ramaiah, 1978) elastic support (Alisjahbana, 2011) , elastic restraint (Szilard, 2004) and elastic support-restraint (Baadilla, 2006). In this study, using deflection for thin plate using free vibration with the modified Bolotin method (Alisjahbana & Wangsadinata, 2015; Bolotin, 1960; Elishakoff, 1976) and modified Bovo-Savoia's equation with multiline equation (linear-quadratic-sextic-linear equation).

2. Governing equation

Based on the classical theory for small amplitude free vibrations of thin plates, the orthotropic thicknesses h, a and b are dimensions along the x and y axes, respectively (Alisjahbana & Wangsadinata, 2015), see Fig. 1 and Fig. 6. The deflection of the orthotropic concrete plate is determined by the following differential equation:

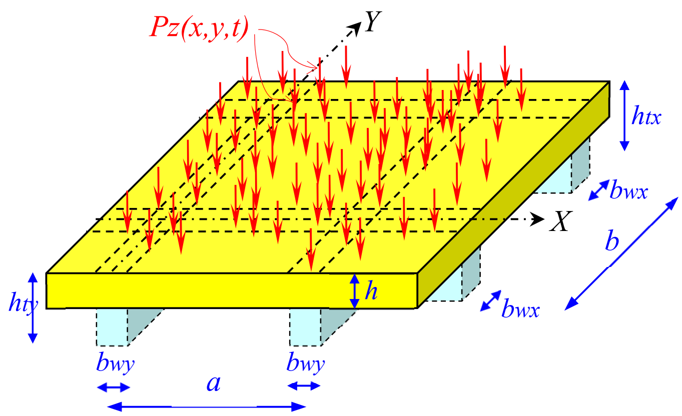

Fig. 1. Load on plate (Szilard, 2004)

$$D_x\left(\frac{\partial^4 w(x,y,t)}{\partial x^4}\right)+2B\left(\frac{\partial^4 w(x,y,t)}{\partial x^2\partial y^2}\right)+D_y\left(\frac{\partial^4 w(x,y,t)}{\partial y^4}\right)+\rho h\frac{\partial^2 w(x,y,t)}{\partial t^2}+\gamma h\frac{\partial w(x,y,t)}{\partial t}=p_z(x,y,t) \qquad (1)$$

where B is the torsional rigidity of the plates, D_x and D_y are the bending rigidities of the plates in the x and y direction, h is the plate thickness, γ is the damping ratio, ρ is the mass density, $w(x,y,t)$ is the deflection vertical; $p_z(x,y,t)$ = dynamic vertical seismic load on the plate

$$D_x=\frac{E_x h^3}{12(1-\nu_x\nu_y)};\ D_y=\frac{E_y h^3}{12(1-\nu_x\nu_y)};\ B=\sqrt{D_x D_y} \qquad (2)$$

where ν_x and ν_y are the Poisson's ratio, E_x and E_y are the Young moduli along x and y respectively, and

$$P_z(x,y,t)=\alpha_{max}(t)P_{grav} \qquad (3)$$

3. Boundary condition

The boundary conditions for all supported are different, depending on the type of supported and the position of x-direction and y-direction, (shown in Fig. 2).

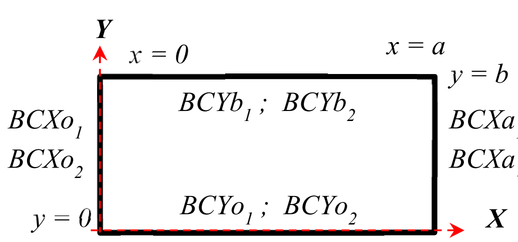

Fig. 2. General boundary conditions.
General boundary conditions (Szilard, 2004)

$$w=0 \qquad (4)$$

$$\frac{\partial w}{\partial x}=0 \qquad (5)$$

$$\frac{\partial^2 w}{\partial x^2}+\nu_y\frac{\partial^2 w}{\partial y^2}=0 \tag{6}$$

$$\left[\frac{\partial^3 w}{\partial x^3}+\left(2-\nu_y\right)\frac{\partial^3 w}{\partial x\partial y^2}\right]=0 \tag{7}$$

$$D_x\left[\frac{\partial^3 w}{\partial x^3}+\left(2-\nu_y\right)\frac{\partial^3 w}{\partial x\partial y^2}\right]-kx\ (w)=0 \tag{8}$$

$$D_x\left(\frac{\partial^2 w}{\partial x^2}+\nu_y\frac{\partial^2 w}{\partial y^2}\right)+cx\ \left(\frac{\partial w}{\partial x}\right)=0 \tag{9}$$

Table 1. Boundary conditions for all support

Type of support		Mathematical expressions		Location
Clamped	1	$w=0$	;	x = 0, x = a
	2	$\frac{\partial w}{\partial x}=0$	;	x = 0, x = a
Simply	1	$w=0$	;	x = 0, x = a
	2	$\frac{\partial^2 w}{\partial x^2}+\nu_y\frac{\partial^2 w}{\partial y^2}=0$	;	x = 0, x = a
Free	1	$\frac{\partial^2 w}{\partial x^2}+\nu_y\frac{\partial^2 w}{\partial y^2}=0$	;	x = 0, x = a
	2	$\left[\frac{\partial^3 w}{\partial x^3}+\left(2-\nu_y\right)\frac{\partial^3 w}{\partial x\partial y^2}\right]=0$	;	x = 0, x = a
ES	1	$\frac{\partial^2 w}{\partial x^2}+\nu_y\frac{\partial^2 w}{\partial y^2}=0$	;	x = 0, x = a
	2	$D_x\left[\frac{\partial^3 w}{\partial x^3}+\left(2-\nu_y\right)\frac{\partial^3 w}{\partial x\partial y^2}\right]-k_x(w)=0$	;	x = 0 (k_x=k_{xo}), x = a (k_x = k_{xa})
ER	1	$w=0$	;	x = 0, x = a
	2	$D_x\left(\frac{\partial^2 w}{\partial x^2}+\nu_y\frac{\partial^2 w}{\partial y^2}\right)+c_x\left(\frac{\partial w}{\partial x}\right)=0$	;	x = 0 (c_x = c_{xo}), x = a (c_x = c_{xa})
ESR	1	$D_x\left[\frac{\partial^3 w}{\partial x^3}+\left(2-\nu_y\right)\frac{\partial^3 w}{\partial x\partial y^2}\right]-k_x(w)=0$	;	x = 0 (k_x=k_{xo}), x = a (k_x = k_{xa})
	2	$D_x\left(\frac{\partial^2 w}{\partial x^2}+\nu_y\frac{\partial^2 w}{\partial y^2}\right)+c_x\left(\frac{\partial w}{\partial x}\right)=0$	;	x = 0 (c_x = c_{xo}), x = a (c_x = c_{xa})

For y-direction similar expressions for an edge at y = 0, y = b.

4. Dynamic response of plates

The dynamic response of the plate (Alisjahbana & Wangsadinata, 2015; Baadilla, 2006) can be found by using the method of separation of variables, which can be written in the following form:

$$\begin{aligned} w(x,y,t)=\sum_{p=1}^{\infty}\sum_{q=1}^{\infty}X_p(x)Y_q(y)\ e^{-\zeta\omega_{pq}t}\left(a_0\ Cos\left(\omega_D\ t\right)+b_0\ Sin\left(\omega_D\ t\right)\right)\ + \\ e^{-\zeta\,\omega_{pq}\,t}\int_0^t\left(\frac{P_z(x,y,t)}{\rho h\,Q_{pq}}\int_{x=0}^{a}X_p(x)dx\int_{y=0}^{b}Y_q(y)dy\cdot\frac{e^{\zeta\,\omega_{pq}\,\tau}}{\omega_D}Sin\left(\omega_D\{t-\tau\}\right)\right)d\tau\Bigg] \end{aligned} \tag{10}$$

where:
a = length of plate in x-direction
b = length of plate in y-direction
ζ = damping ratio = 0.5

ω_{pq} = natural frequency

ω_D = $\omega_{pq}\sqrt{1-\zeta^2}$

Subsitution Eq. (3) to Eq. (10)

$$w(x,y,t)=\sum_{p=1}^{\infty}\sum_{q=1}^{\infty}X_p(x)Y_q(y)\,e^{-\zeta\omega_{pq}t}\left(a_0\,Cos\left(\omega_D\,t\right)+b_0\,Sin\left(\omega_D\,t\right)\right)+$$
$$\left.e^{-\zeta\,\omega_{pq}\,t}\int_0^t\left(\frac{P_{grav}\,\alpha_{max}(\tau)}{\rho\,h\,Q_{pq}}\,X_p(x)Y_q(y)\frac{e^{\zeta\,\omega_{pq}\,\tau}}{\omega_D}Sin\left(\omega_D\{t-\tau\}\right)\right)d\tau\right] \tag{11}$$

$$Q_{pq}=\int_0^a\int_0^b X_p(x)^2\,Y_q(y)^2\,dx\,dy \tag{12}$$

$$X_p(x)=Ax_1\;Cosh\left(\beta x\right)+Ax_2\;Sinh\left(\beta x\right)+Ax_3\;Cos\left(\frac{p\pi}{a}x\right)+Ax_4\;Sin\left(\frac{p\pi}{a}x\right) \tag{13.a}$$

$$Y_q(y)=By_1\;Cosh\left(\theta\,y\right)+By_2\;Sinh\left(\theta\,y\right)+By_3\;cos\left(\frac{q\pi}{b}y\right)+By_4\;sin\left(\frac{q\pi}{b}y\right) \tag{13.b}$$

$$\beta=\sqrt{\left(\frac{p\,\pi}{a}\right)^2+\frac{2B}{D_y}\left(\frac{q\pi}{b}\right)^2} \tag{14.a}$$

$$\theta=\sqrt{\left(\frac{q\pi}{b}\right)^2+\frac{2B}{D_y}\left(\frac{p\pi}{a}\right)^2} \tag{14.b}$$

$$\alpha_{\max}(t)\cdot=\begin{cases}\alpha_1(t) & 0.00\le t\le 0.05\\ \alpha_2(t) & 0.05<t\le 0.15\\ \alpha_3(t) & 0.15<t\le 0.60\\ \alpha_4(t) & t>0.60\end{cases} \tag{15}$$

where $\alpha_{max}(t)$ is multi-line 1-2-6 (linear-quadratic-sextic) equation ,

$$\alpha_1(t)=fa\cdot t+\left(PGAv/g\right) \tag{15.a}$$

$$\alpha_2(t)=fb_0\cdot t^2+fb_1\cdot t+fb_2 \tag{15.b}$$

$$\alpha_3(t)=fc_0\cdot t^6+fc_1\cdot t^5+fc_2\cdot t^4+fc_3\cdot t^3+fc_4\cdot t^2+fc_5\cdot t+fc_6 \tag{15.c}$$

$$\alpha_4(t)=\alpha_3(0.6)\cdot(1.3-0.5t) \tag{15.d}$$

$\alpha_{max}(t)$ can be shown in Fig. 5

Variable fa, fb_0, fb_1, fb_2, fc_0, fc_1, fc_2, fc_3, fc_4, fc_5, fc_6 depends on ($PGAv/g$) for *floor slab* and *near fault* is as following:

$fa = 64.6415\ (PGAv/g)^3 - 53.154\ (PGAv/g)^2 + 44.676\ (PGAv/g)$

$fb_0 = 313.83\ (PGAv/g)^3 - 415.48\ (PGAv/g)^2 + 8.48\ (PGAv/g)$

$fb_1 = -100.45\ (PGAv/g)^3 + 106.22\ (PGAv/g)^2 - 1.9\ (PGAv/g)$

$fb_2 = 7.47\ (PGAv/g)^3 - 6.93\ (PGAv/g)^2 + 3.35\ (PGAv/g)$

$fc_0 = 58.318\ (PGAv/g)^2 + 901.284\ (PGAv/g) - 22.307$

$fc_1 = -133.005\ (PGAv/g)^2 - 2338.617\ (PGAv/g) + 57.818$

$fc_2 = 116.066\ (PGAv/g)^2 + 2528.539\ (PGAv/g) - 62.388$

$fc_3 = -43.659\ (PGAv/g)^2 - 1474.235\ (PGAv/g) + 36.226$

$fc_4 = 1.625\ (PGAv/g)^2 + 500.194\ (PGAv/g) - 12.173$

$fc_5 = 4.529\ (PGAv/g)^2 - 98.943\ (PGAv/g) + 2.337$

$fc_6 = -1.768\ (PGAv/g)^2 + 10.668\ (PGAv/g) - 0.211$

for *floor slab* and *far fault* is as following:

$fa = 56.2\ (PGAv/g)^3 - 59.88\ (PGAv/g)^2 + 47.4015\ (PGAv/g)$

$fb_0 = 1190.4\ (PGAv/g)^3 - 1256.4\ (PGAv/g)^2 + 75.63\ (PGAv/g)$

$fb_1 = -260.65\ (PGAv/g)^3 + 275.74\ (PGAv/g)^2 - 20.58(PGAv/g)$

$fb_2 = 12.87\ (PGAv/g)^3 - 13.64\ (PGAv/g)^2 + 4.21\ (PGAv/g)$

$$fc_0 = 2.4811\ (PGAv/g)^2 + 890.103\ (PGAv/g) + 14.096$$
$$fc_1 = -\ 9.4219\ (PGAv/g)^2 - 2299.332\ (PGAv/g) - 36.423$$
$$fc_2 = 14.757\ (PGAv/g)^2 + 2470.543\ (PGAv/g) + 39.149$$
$$fc_3 = -\ 12.627\ (PGAv/g)^2 - 1427.031\ (PGAv/g) - 22.627$$
$$fc_4 = 6.553\ (PGAv/g)^2 + 476.874\ (PGAv/g) + 0.570$$
$$fc_5 = -\ 2.175\ (PGAv/g)^2 - 91.677\ (PGAv/g) - 1.46$$
$$fc_6 = 0.5015\ (PGAv/g)^2 + 9.212\ (PGAv/g) + 0.149$$

$$w_{pq}(t) = e^{-\zeta\,\omega_{pq}\,t} \int_0^t \left(\frac{P_{grav}\,\alpha_{max}(\tau)}{\rho\, h\, Q_{pq}}\, X_p(x) Y_q(y) \frac{e^{\zeta\,\omega_{pq}\,\tau}}{\omega_D} Sin\left(\omega_D\{t-\tau\}\right) \right) d\tau \tag{16}$$

$$v_{pq}(t) = \frac{w_{pq}(t)}{\partial t} \tag{17}$$

$$a_0 = w_{pq}(0) \tag{18}$$

$$b_0 = \frac{\zeta \cdot \omega_{pq}\, w_{pq}(0) + v_{pq}(0)}{\omega_D} \tag{19}$$

The graphic of Bovo-Savoia's equation from *PGAv* = 0.1 g to *PGAv* = 1.0 g and dynamic vertical seismic load multiline 1-2-6 (linear-quadratic-sextic) equation, from *PGAv* = 0.1 g to *PGAv* = 1.0 g, shown in Fig. 3 and Fig. 4.

Table 2. R^2 of Multiline 1-2-6's equation vs Bovo-Savoia's equation

PGAv/g	Near	Far
0.10	0.999997	0.998544
0.20	0.999991	0.999989
0.30	0.999953	0.999951
0.40	0.999986	0.999984
0.50	0.999999	0.999999
0.60	0.999992	0.999995
0.70	0.999989	0.999994
0.80	0.999999	0.999999
0.90	0.999980	0.999987
1.00	0.999833	0.999917

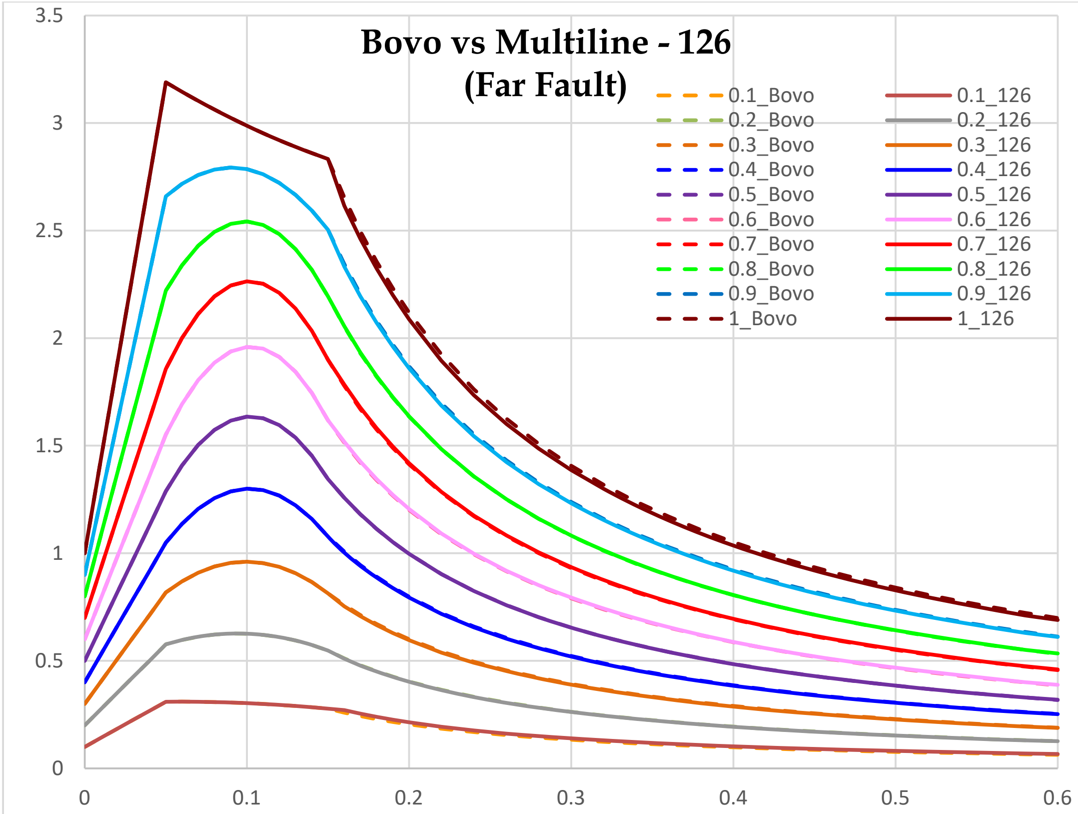

Fig. 3. Far Fault Bovo-Savoia's vs Multiline 1-2-6

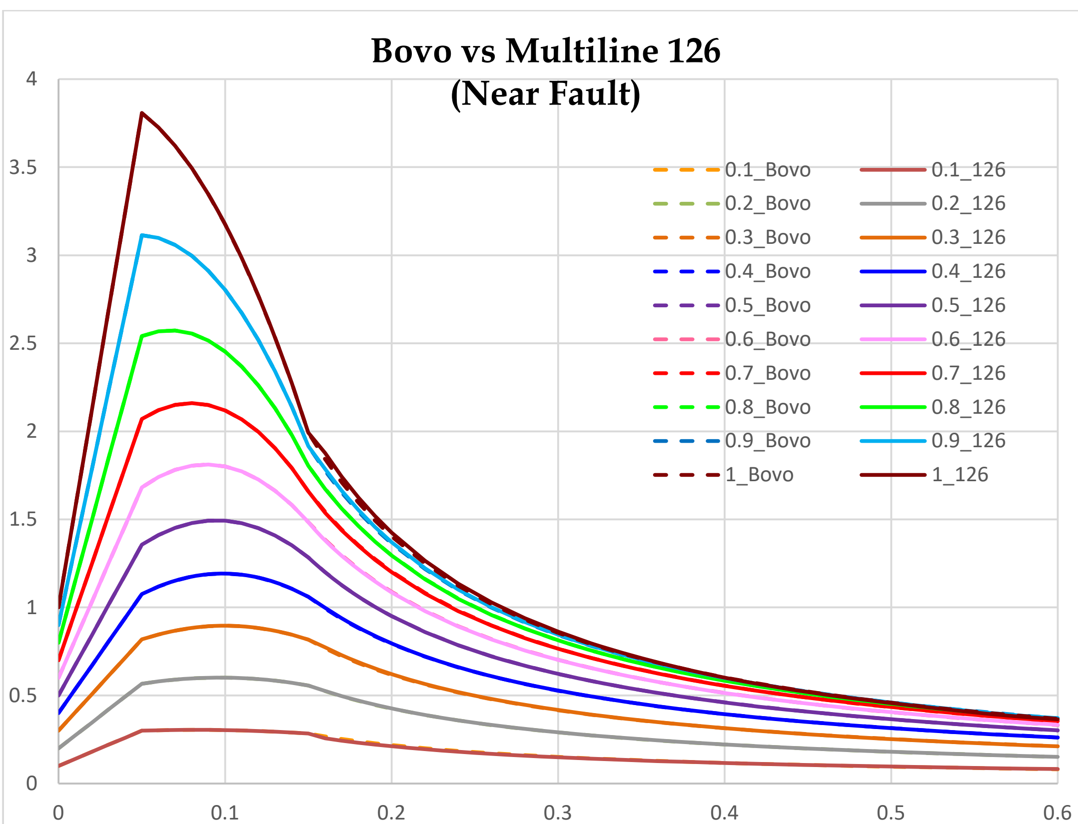

Fig. 4. Near fault Bovo-Savoia's vs Multiline1-2-6

$\alpha_2(t)$

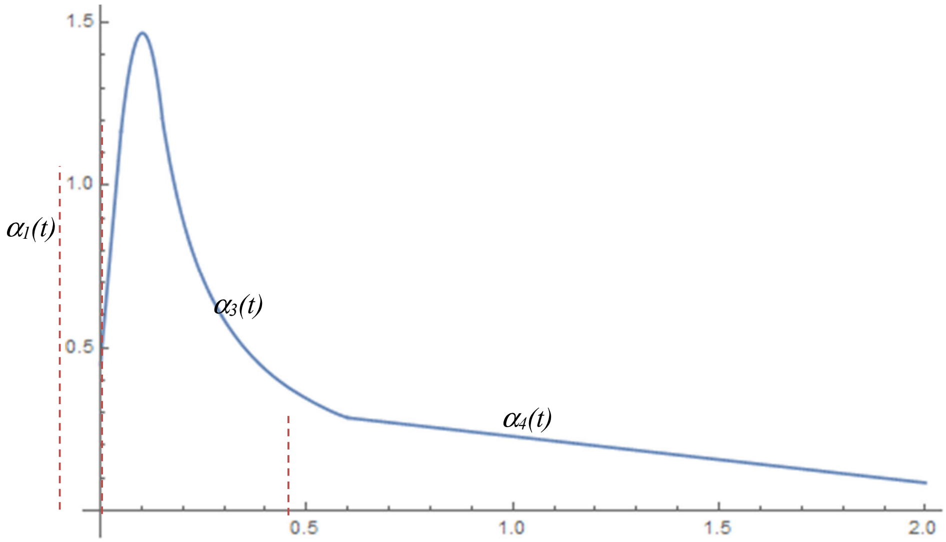

Fig. 5. $a_{max}(t)$ for PGAv = 0.45 g and Far fault

Bovo-Savoia's equation modified into equation multiline 1-2-6, for this case PGAv = 0.45 g and fault is far substitute to equation (shown in Fig. 5), the dynamic vertical seismic load is become:

$$a_1(t) = 0.45 + 14.3326\, t$$
$$a_2(t) = 0.305179 + 22.8246\, t - 111.912\, t^2$$
$$a_3(t) = 4.39571 - 43.155\, t + 223.491\, t^2 - 667.348\, t^3 + 1153.88\, t^4 - 1073.03\, t^5 + 415.145\, t^6$$
$$a_3(0.6) = 0.285428$$
$$a_4(t) = 0.285428\, (1.3 - 0.5\, t)$$

5. Results and discussion

Data parameter for orthotropic plate with vertical seismic load as follows, (Alisjahbana & Wangsadinata, 2015).

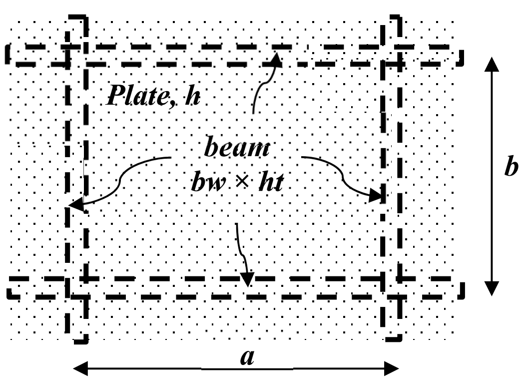

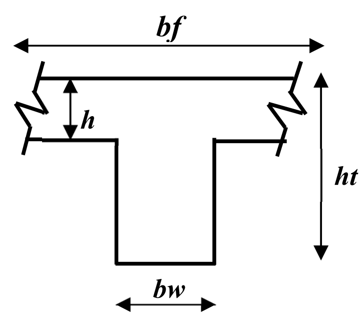

(a) (b)

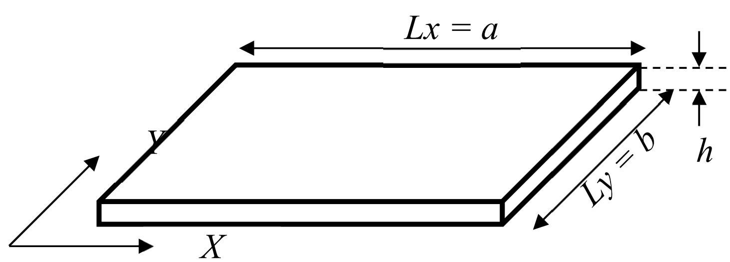

(c)

Fig. 6. Dimension of plate

a = 5 m, b = 3.5 m , h = 0.25 m, bf = 1.25 m, bw = 0.3 m , ht = 0.75 m, ρ = 2500 kg/m³, ζ = 0.05, $x_0 = a/2$, $y_0 = b/2$, E_x = 2.7×10^9 N/m², E_y = 2.25×10^9 N/m², v_y = 0.15, v_x = 0.18,

$k_{xy} = (384\ EI / 5\ L^4)$, $c_{xy} = (G\ J / Lx)/Ly$, (Salmon;et-al, 2009),
$k_{xo} = k_{xa} = 6.30545\times10^6$ N/m/m, $k_{yo} = k_{yb} = 1.93197\times10^6$ N/m/m,
$c_{xo} = c_{xa} = 665\ 944$ N-m/rad/m, $c_{yo} = c_{yb} = 547\ 813$ N-m/rad/m.
$PGAv = 0.45$ g, Fault = "FAR", LL = 4000 N/m²; DL = h×23.5×1000 N/m²; SIDL = 1000 N/m².
P_{max} = (1.2× (DL + SIDL) + 1.6×LL) = 14650 N/m².

5.1 Displacement

The resume of dynamic displacement for all supported, (Table 3) respectively:

Table 3. Displacement all support

Support	Deflect max	tmax	Figure
Free edge	0.000117051	0.104	Fig. 7
Clamp	0.000728537	0.180	Fig. 8
Simply	0.00226828	0.180	Fig. 9
ES (elastic support)	0.00181305	0.184	Fig. 10
ER (elastic restraint)	0.00333596	0.152	Fig. 11
ESR (elastic support-restraint)	0.00539299	0.164	Fig. 12

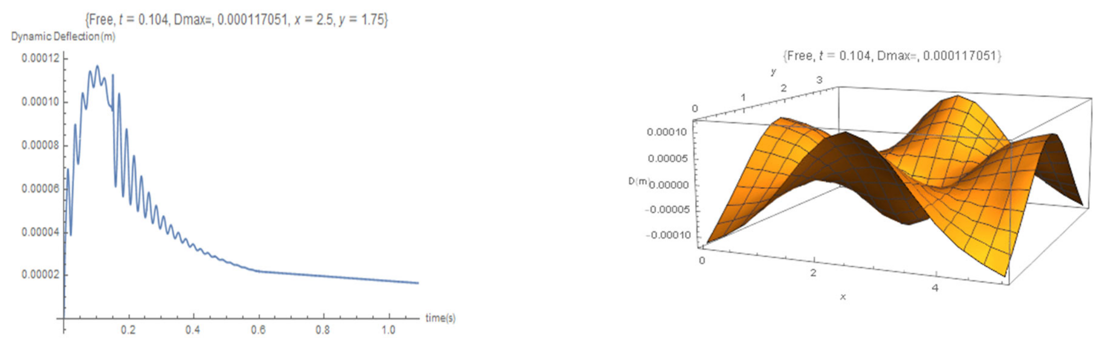

(a) 2 D (b) 3D

Fig. 7. Graphic 2D & 3D dynamic deflection at t = 0.104 second for free edge

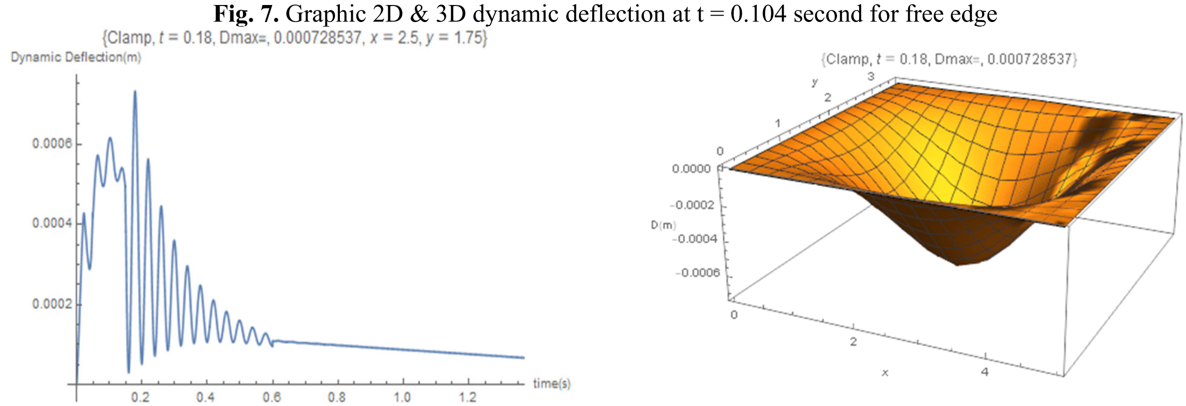

(a) 2 D (b) 3D

Fig. 8. Graphic 2D & 3D dynamic deflection at t = 0.180 second for clamp supported

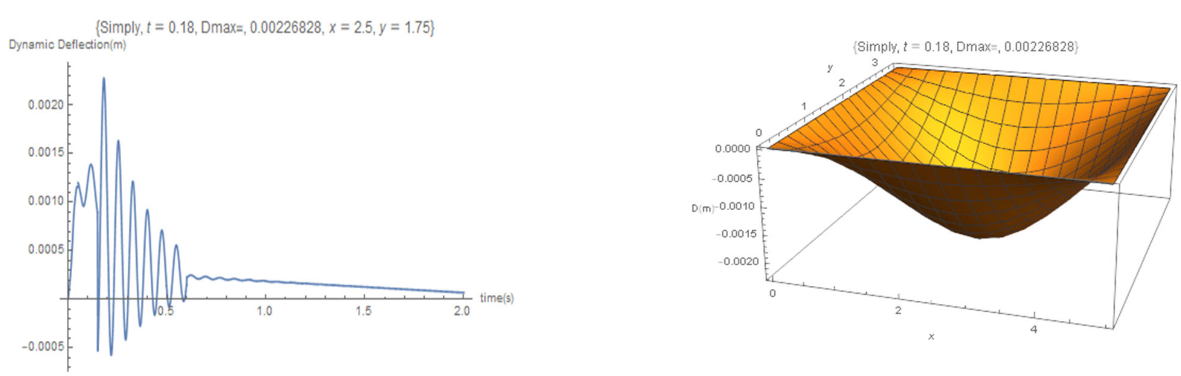

(a) 2 D (b) 3D

Fig. 9. Graphic 2D & 3D dynamic deflection at t = 0.180 second for simply supported

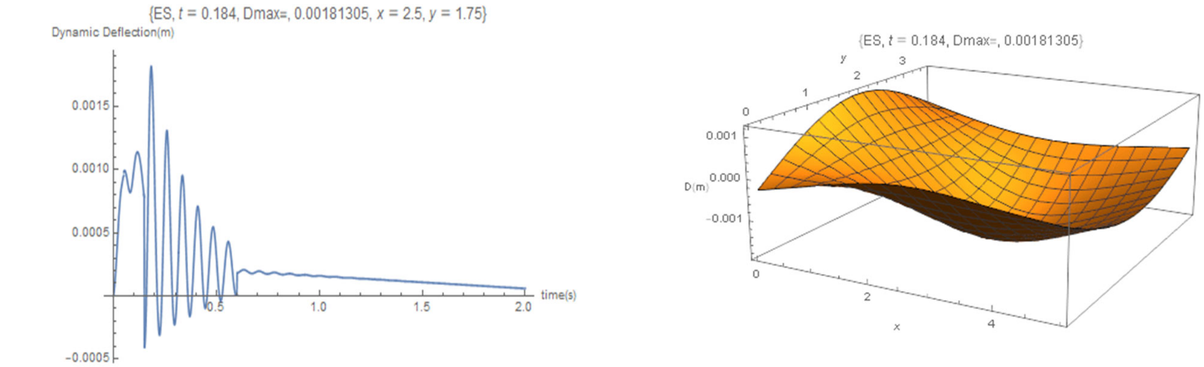

(a) 2 D (b) 3D

Fig. 10. Graphic 2D & 3D dynamic deflection at t = 0.184 second for ES (elastic support)

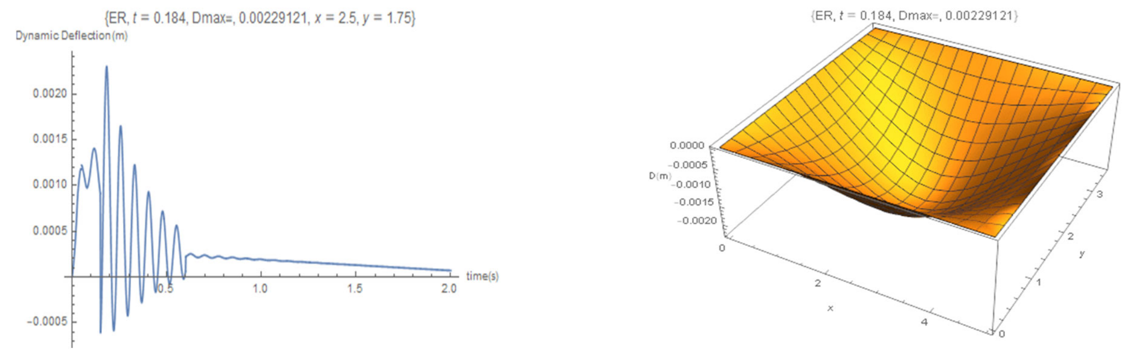

(a) 2 D (b) 3D

Fig. 11. Graphic 2D & 3D dynamic deflection at t = 0.184 second for ER (elastic restraint)

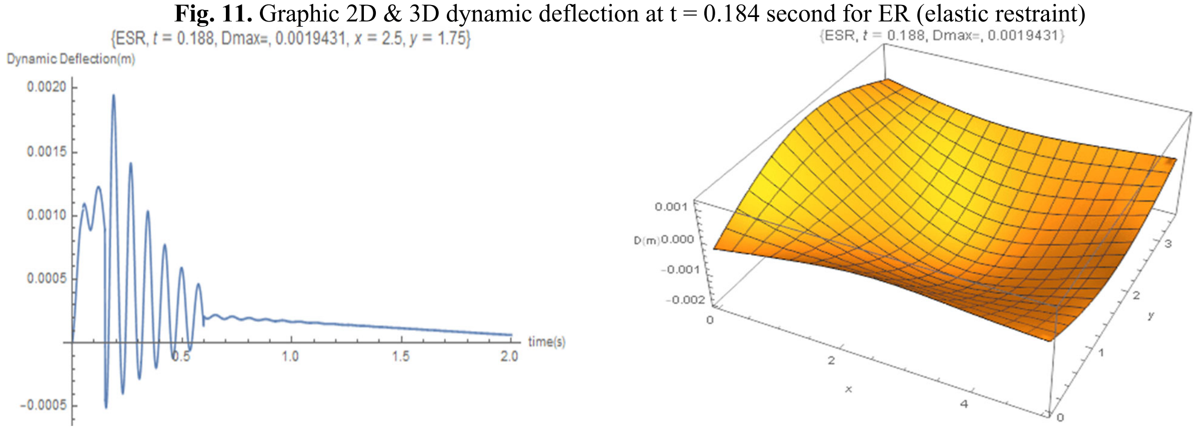

(a) 2 D (b) 3D

Fig. 12. Graphic 2D & 3D dynamic deflection at t = 0.188 second for ESR (elastic support-restraint)

Table 4. Summary of dynamic deflection (m)

X	Y	Free	Clamp	Simply	ES	ER	ERS
0	0	0.0001116	0	0	0.0002598	0	0.0002307
0	1/4b	0	0	0	-0.0007051	0	-0.0007582
0	1/2b	-0.0000896	0	0	-0.0012027	0	-0.0012184
0	3/4b	0	0	0	-0.0009614	0	-0.0009480
0	b	0.0001116	0	0	-0.0002497	0	-0.0002588
1/4a	0	0	0	0	-0.0001387	0	-0.0001547
1/4a	1/4b	0	0.0001925	0.0010486	0.0003775	0.0011409	0.0005023
1/4a	1/2b	-0.0000170	0.0003515	0.0014915	0.0006400	0.0015630	0.0008001
1/4a	3/4b	0	0.0001925	0.0010486	0.0005590	0.0010597	0.0006702
1/4a	b	0	0	0	0.0001771	0	0.0002155
1/2a	0	-0.0001181	0	0	-0.0004090	0	-0.0003881
1/2a	1/4b	0	0.0003727	0.0015517	0.0010380	0.0016258	0.0011886
1/2a	1/2b	0.0001171	0.0007285	0.0022683	0.0018131	0.0022912	0.0019431
1/2a	3/4b	0	0.0003726	0.0015517	0.0014623	0.0015147	0.0015209

1/2a	b	-0.0001181	0	0	0.0003954	0	0.0004272
3/4a	0	0	0	0	-0.0002837	0	-0.0002545
3/4a	1/4b	0	0.0001925	0.0010486	0.0010002	0.0010551	0.0011007
3/4a	1/2b	-0.0000170	0.0003516	0.0014915	0.0016215	0.0014464	0.0016775
3/4a	3/4b	0	0.0001925	0.0010486	0.0013085	0.0009802	0.0013072
3/4a	b	0	0	0	0.0003063	0	0.0003203
a	0	0.0001116	0	0	-0.0001081	0	-0.0000996
a	1/4b	0	0	0	0.0005199	0	0.0005766
a	1/2b	-0.0000896	0	0	0.0008029	0	0.0008397
a	3/4b	0	0	0	0.0006236	0	0.0006266
a	b	0.0001116	0	0	0.0001057	0	0.0001138

5.2 Dynamic bending moment

The result of dynamic bending moment of plate for X-direction, Y-direction, respectively:
Free edge (Fig. 13), Clamped (Fig. 14), Simply support (Fig. 15), Elastic support (Fig. 16), Elastic Restraint (Fig. 17), Elastic support-restraint (Fig. 18).

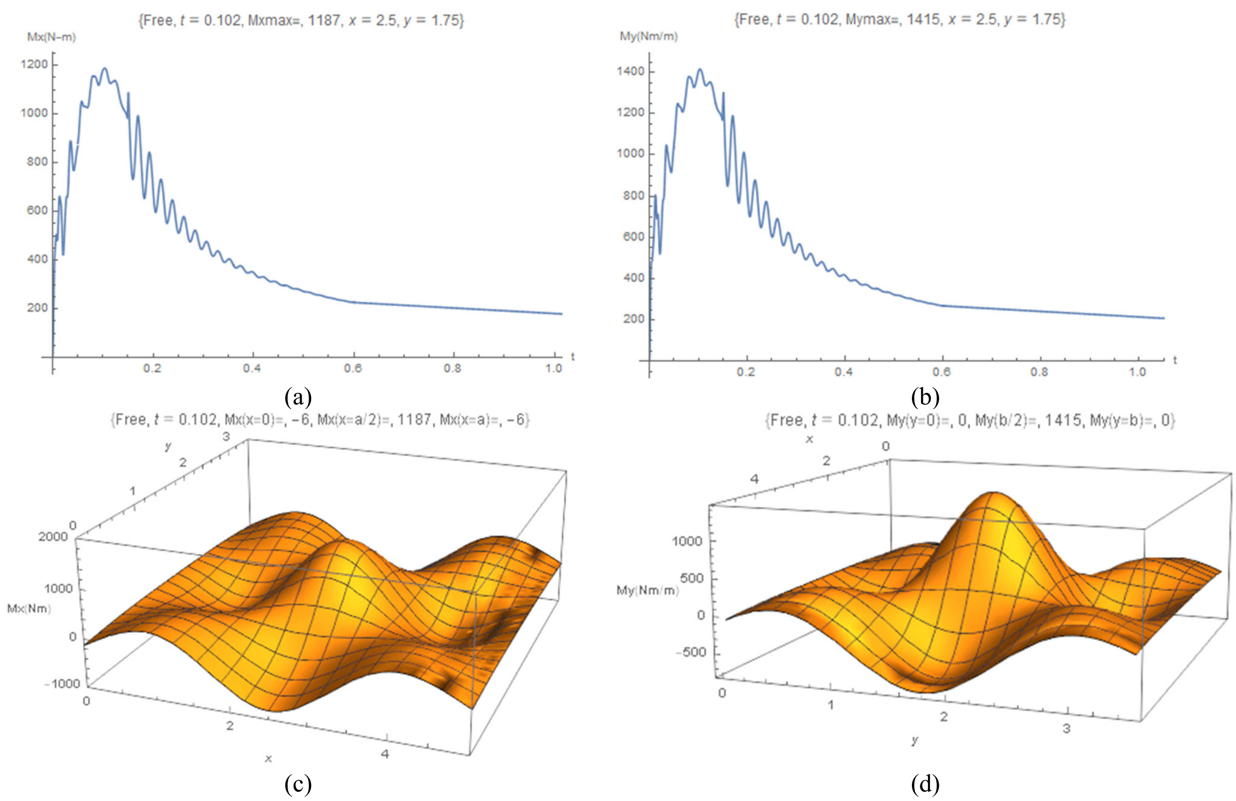

Fig. 13. Dynamic bending moment (a) 2D in X-dir, (b) 2D -Y-dir, (c) 3 D – Xdir, (d) 3D – Ydir for free edge

Table 5. Mx and My at free edge (Fig. 13)

$Mx_{(x=0)}$ =	-6	$My_{(y=0)}$ =	0
$Mx_{(x=a/2)}$ =	1187	$My_{(y=b/2)}$ =	1415
$Mx_{(x=a)}$ =	-6	$My_{(y=b)}$ =	0
$Mx_{(y=0)}$ =	-810	$My_{(x=0)}$ =	-770
$Mx_{(y=b)}$ =	-810	$My_{(x=a)}$ =	-770
tx_{max} =	0.102	ty_{max} =	0.102

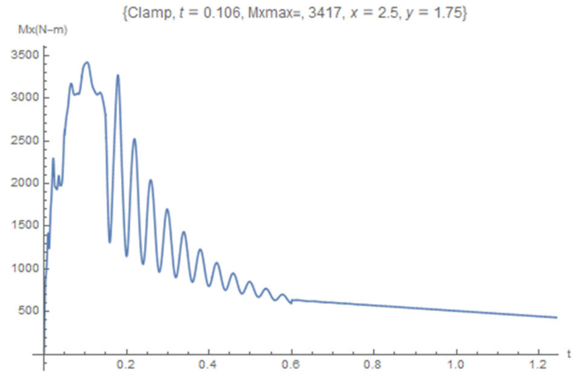

(a)

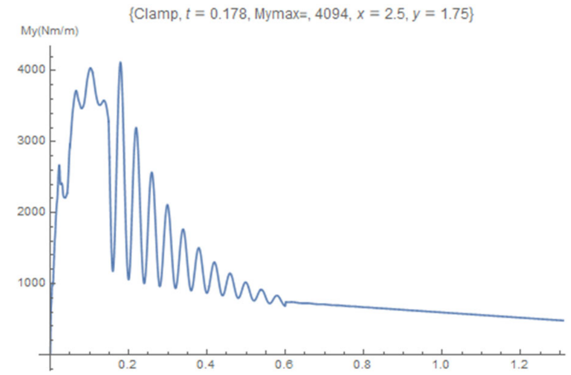

(b)

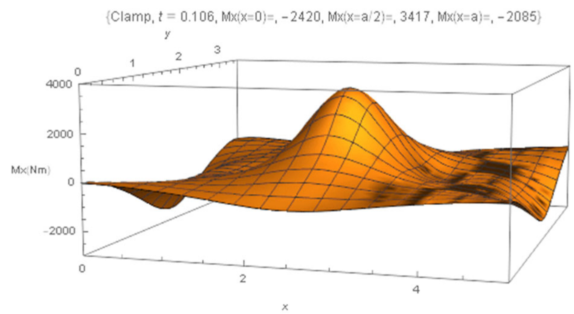

(c)

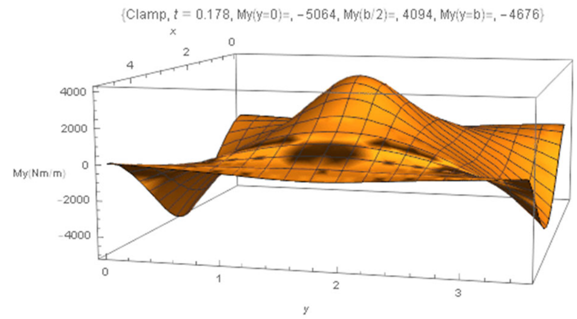

(d)

Fig. 14. Dynamic bending moment (a) 2D in X-dir, (b) 2D -Y-dir, (c) 3 D – Xdir, (d) 3D – Ydir for clamp supported.

Table 6. Mx and My at clamp supported (Fig. 14)

$Mx_{(x=0)}$ =	-2,420	$My_{(y=0)}$ =	-5064
$Mx_{(x=a/2)}$ =	3,417	$My_{(y=b/2)}$ =	4094
$Mx_{(x=a)}$ =	-2,085	$My_{(y=b)}$ =	-4676
$Mx_{(y=0)}$ =	-712	$My_{(x=0)}$ =	-508
$Mx_{(y=b)}$ =	-722	$My_{(x=a)}$ =	-510
tx_{max} =	0.106	ty_{max} =	0.178

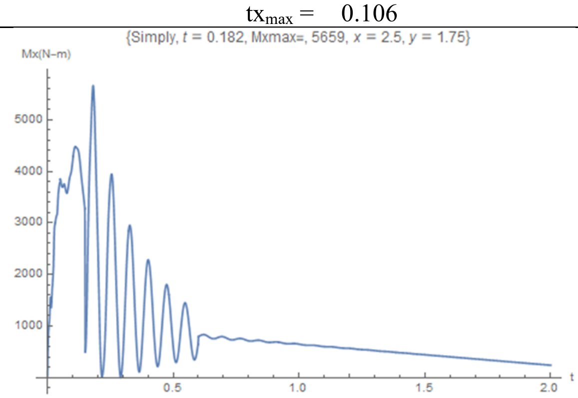

(a)

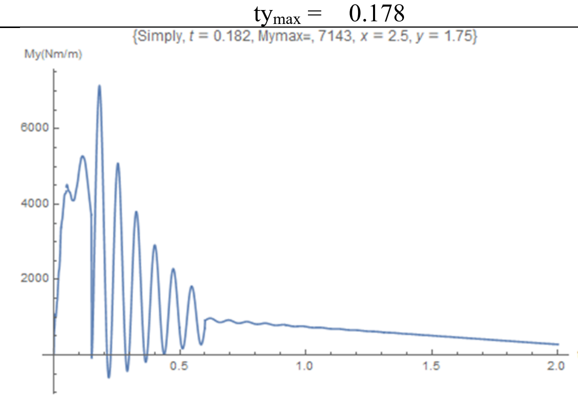

(b)

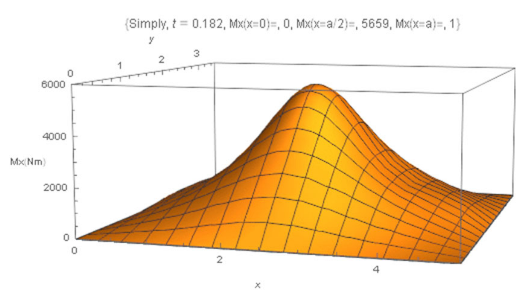

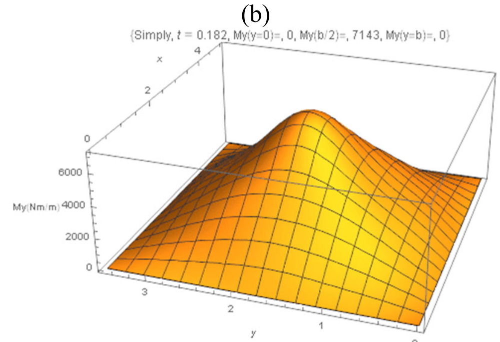

(c) (d)

Fig. 15. Dynamic bending moment (a) 2D in X-dir, (b) 2D -Y-dir, (c) 3 D – Xdir, (d) 3D – Ydir for simply supported

Table 9. Mx and My at symply supported (Fig. 15)

$Mx_{(x=0)}$ =	0	$My_{(y=0)}$ =	0
$Mx_{(x=a/2)}$ =	5,659	$My_{(y=b/2)}$ =	7143
$Mx_{(x=a)}$ =	1	$My_{(y=b)}$ =	0
$Mx_{(y=0)}$ =	0	$My_{(x=0)}$ =	0
$Mx_{(y=b)}$ =	0	$My_{(x=a)}$ =	1
tx_{max} =	0.106	ty_{max} =	0.182

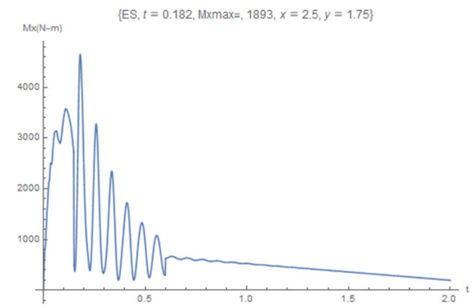

(a)

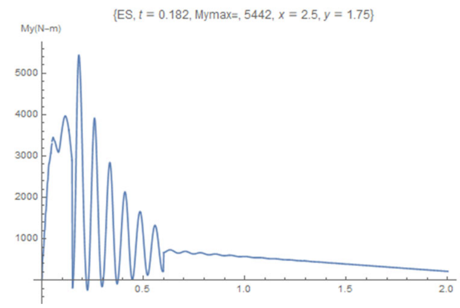

(b)

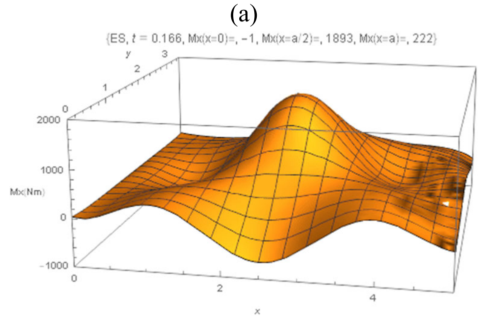

(c)

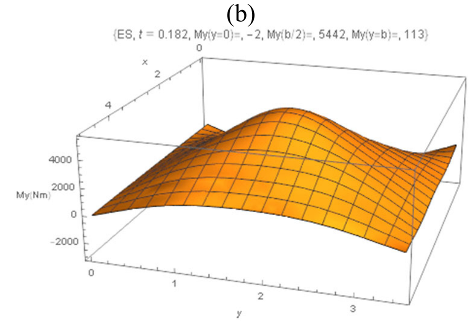

(d)

Fig. 16. Dynamic bending moment (a) 2D in X-dir, (b) 2D -Y-dir, (c) 3 D – Xdir, (d) 3D – Ydir for ES (elastic support)

Table 8. Mx and My at ES (figure 16)

$Mx_{(x=0)}$ =	-2	$My_{(y=0)}$ =	-2
$Mx_{(x=a/2)}$ =	4,635	$My_{(y=b/2)}$ =	5442
$Mx_{(x=a)}$ =	209	$My_{(y=b)}$ =	113
$Mx_{(y=0)}$ =	-1,217	$My_{(x=0)}$ =	-3115
$Mx_{(y=b)}$ =	785	$My_{(x=a)}$ =	1688
tx_{max} =	0.106	ty_{max} =	0.182

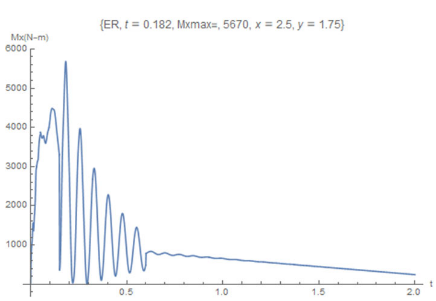

(a)

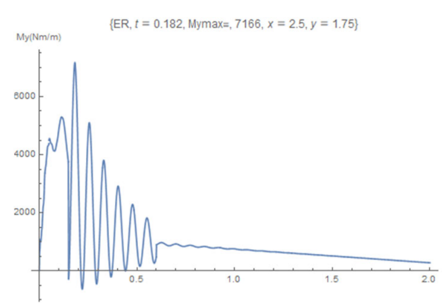

(b)

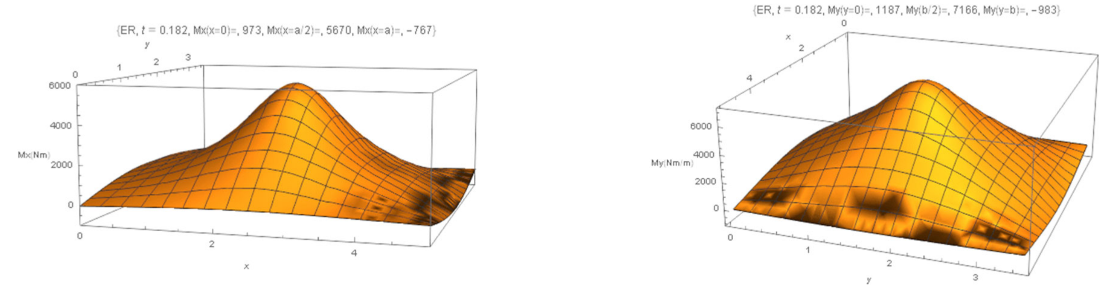

(c) (d)

Fig. 17. Dynamic bending moment (a) 2D in X-dir, (b) 2D -Y-dir, (c) 3 D – Xdir, (d) 3D – Ydir for ER (elastic restraint).

Table 9. Mx and My at ER (figure 17)

$Mx_{(x=0)}$ =	973	$My_{(y=0)}$ =	1187
$Mx_{(x=a/2)}$ =	5,670	$My_{(y=b/2)}$ =	7166
$Mx_{(x=a)}$ =	-767	$My_{(y=b)}$ =	-983
$Mx_{(y=0)}$ =	214	$My_{(x=0)}$ =	146
$Mx_{(y=b)}$ =	-176	$My_{(x=a)}$ =	-115
tx_{max} =	0.106	ty_{max} =	0.182

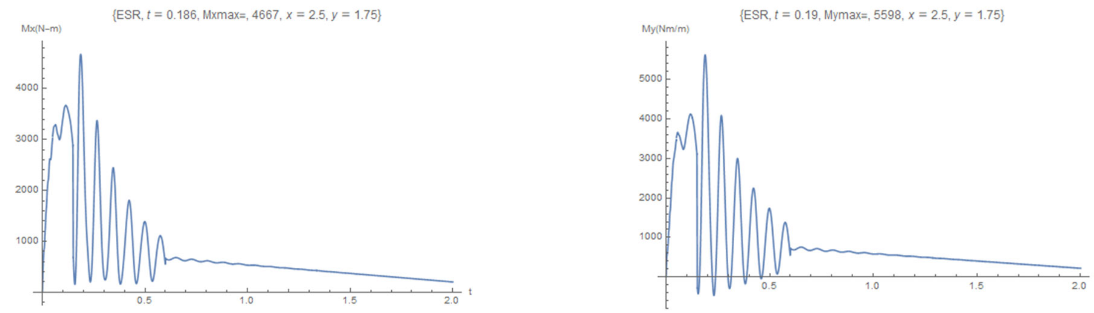

(a) (b)

(c) (d)

Fig. 18. Dynamic bending moment (a) 2D in X-dir, (b) 2D -Y-dir, (c) 3 D – Xdir, (d) 3D – Ydir for ESR (elastic support-restraint).

Table 10. Mx and My at ESR (Fig. 18)

$Mx_{(x=0)}$ =	1,219	$My_{(y=0)}$ =	1129
$Mx_{(x=a/2)}$ =	4,667	$My_{(y=b/2)}$ =	5598
$Mx_{(x=a)}$ =	-224	$My_{(y=b)}$ =	-592
$Mx_{(y=0)}$ =	-896	$My_{(x=0)}$ =	-2791
$Mx_{(y=b)}$ =	656	$My_{(x=a)}$ =	1915
tx_{max} =	0.106	ty_{max} =	0.19

5.3 Flexural stress

Flexural stress on the plates due to dynamic vertical seismic loads with each support is shown in figures 19(a), 19(b), 19(c), 19(d), 19(e) and 19(f).

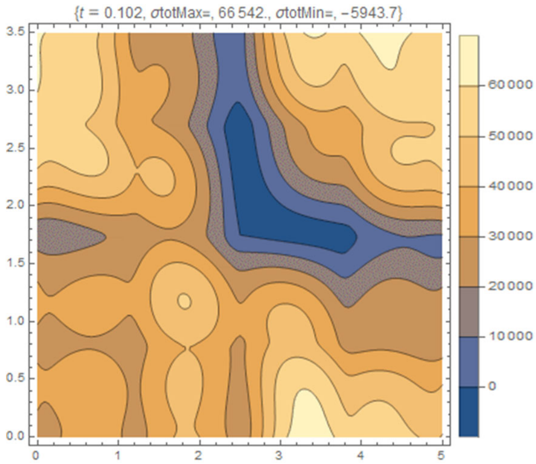

(a) Free edge

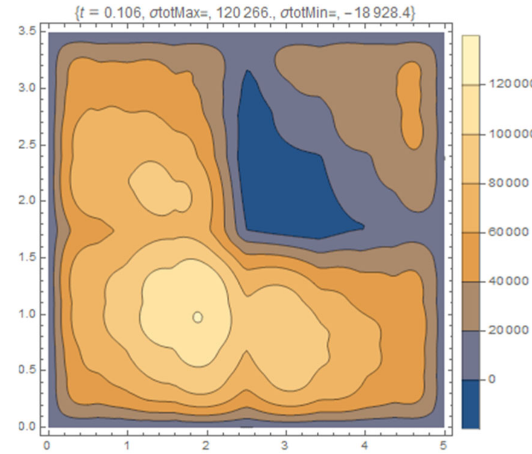

(b) Clamp

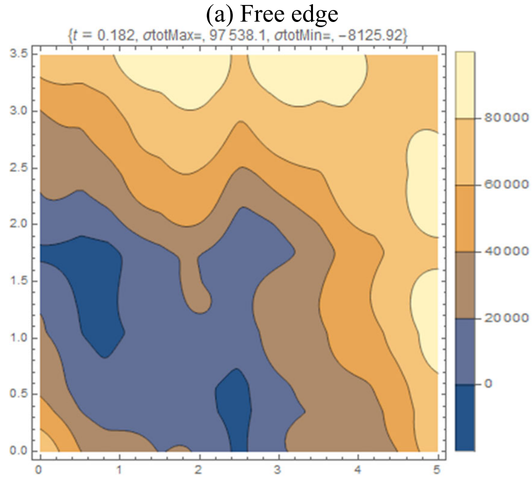

(c) Simply

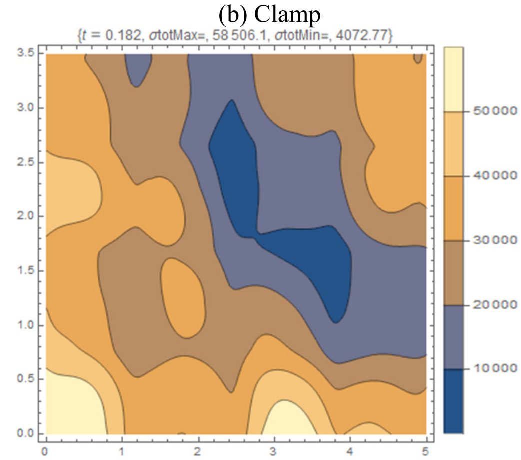

(d) Elastic support

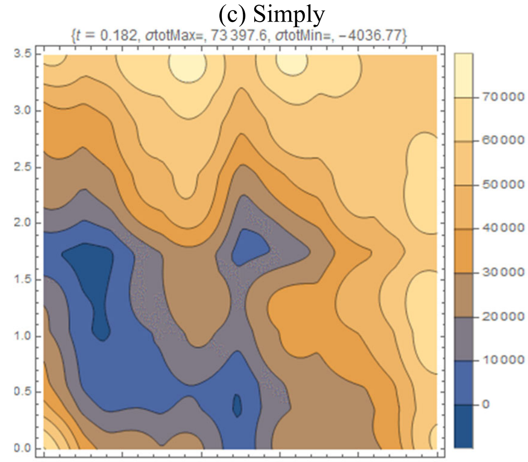

(e) Elastic restraint

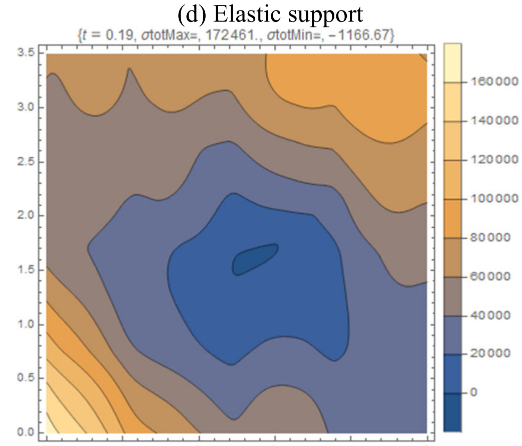

(f) Elastic support – restraint

Fig. 19. Flexural stress for all sides with support

Table 11. Flexural stress for all sides with support

Stress	free	clamp	simply	ES	ER	ESR	unit
σtotMax	66,542	120,266	97,538	58,506	73,398	172,461	N/mm²
σtotMin	-5,944	-18,928	-8,126	4,073	-4,037	-1,167	N/mm²
t at	0.102	0.106	0.182	0.182	0.182	0.19	second

6. Conclusion

1) Dynamic vertical seismic loads for plates if $t < 0.05$ using linear equation, $0.05 \leq t < 0.15$ using quadratic equation, $0.15 \leq t \leq 0.6$ using sextic equation, and for $t > 0.6$ using linear line.

2) Integral calculation using sextic equation faster than using power equation (x^{-t}).
3) The theoretical modelling is clamped, simply supported and free edge, real modelling is ESR, ER and ES. Flexural stress contour Clamped ≈ ESR, simply ≈ ER, free edge ≈ ES.
4) The support type should use ESR in this case, because the edge support has rotation and translation, but to simplify the calculation process. calculations can use clamped support, increasing the calculation results in the middle of the span value by 30% (Clamped/ESR = 4094/5598 = 73%). While in the support area positive moments and negative moments are needed, given the dynamic vertical seismic load, the value of positive moments and negative moments in edge is only 50% of the calculation with clamped analysis. (ESR/Clamp = 1219/2420 = 50.37%).
5) If this case assumes ER support, then the calculation will be simplified if it is used simply supported because the value simply supported ≈ ER is for the center of the span while the edge support requires positive moments and negative moments of 20% (ER negative /ER positive = 17.16%)
6) whereas if this case assumes ES support, you cannot use the free edge calculation, because the free edge value is relatively small compared to ES support (free/ES = 1187/4635 =25.61%), but will use the simple support assumption, because the positive moment is more than 100 % (Simplify/ ES = 5657/4635 =122%) , and moment of edge support= 0 (ES = simplify = 0)

References

ACI-318M-14. (2014). *Building Code Requirements for Structural Concrete (ACI 318S-14) and Commentary (ACI 318SR-14)*. American Concrete Institute.

ACI 318-63. (1963). *Building Code Requirements for Reinforced Concrete*. ACI American Concrete Institute.

Alisjahbana, S. W. (2011). *Dinamika Struktur Pelat*. Universitas Bakrie.

Alisjahbana, S. W., & Wangsadinata, W. (2015). Dynamic Response of Rigid Roadway Pavements. In S. Saha, N. Lloyd, S. Yazdani, & A. Singh (Eds.), *Sustainable Solutions in Structural Engineering and Construction* (pp. 1–7). ISEC Press. https://www.researchgate.net/publication/287533301

Baadilla, D. A. (2006). *Dinamika Pelat Perkerasan kaku dengan tahanan tepi sembarang*. Universitas Tarumanagara.

Berkeley.edu. (n.d.). *https://ngawest2.berkeley.edu/*. https://ngawest2.berkeley.edu/

Bolotin, V. V. (1960). *Statistical theory of the aseismic design of structures* (pp. 1365–1374).

Bovo, M., & Savoia, M. (2019). Evaluation of force fluctuations induced by vertical seismic component on reinforced concrete precast structures. *Engineering Structures*, *178*(March 2018), 70–87. https://doi.org/10.1016/j.engstruct.2018.10.018

BS8110. (1997). *Structural use of concrete — Part 1 : Code of practice for design and Construction*. British Standard.

Elishakoff. (1974). Vibration Analysis of Clamped Square Orthotropic Plate. *AIAA JOURNAL*, *12*(No 7), 921–9244.

Elishakoff. (1976). *Bolotins Dynamic Edge Effect Method*. 95–104. https://doi.org/10.1177/058310247600800109

PBI. (1971). *Peraturan Beton Bertulang Indonesia 1971* (Vol. 7). Direktorat Penyelidikan Masalah Bangunan.

Salmon;et-al. (2009). *Steel Structures Design and Behavior 5th*. Pearson Prentice Hall.

SNI 2847:19. (2019). *Persyaratan beton struktural untuk bangunan gedung dan penjelasan*. Badan Standardisasi Nasional.

Szilard, R. (2004). *Theories and Applications of Plate Analysis: Classical, Numerical and Engineering Methods* (Vol. 57). John Wiley & Sons, Inc. https://doi.org/10.1115/1.1849175

Vijayakumar, K. (1974). Natural frequencies of rectangular orthotropic plates with a pair of parallel edges simply supported. *Journal of Sound and Vibration*, *35*(3), 379–394. https://doi.org/10.1016/0022-460X(74)90067-4

Vijayakumar, K., & Ramaiah, G. K. (1978). Analysis of vibration of clamped square plates by the Rayleigh-Ritz method with asymptotic solutions from a modified Bolotin method. *Journal of Sound and Vibration*, *56*(1), 127–135. https://doi.org/10.1016/0022-460X(78)90575-8

Zhu, X. Q., & Law, S. S. (2003). Dynamic Behavior of Orthotropic Rectangular Plates under Moving Loads. *Journal of Engineering Mechanics*, *129*(1), 79–87. https://doi.org/10.1061/(asce)0733-9399(2003)129:1(79)